

THE STELLAR CONTENT OF THE NUCLEI OF LATE-TYPE SPIRAL GALAXIES

JAY A. FROGEL

Cerro Tololo Inter-American Observatory,¹ National Optical Astronomy Observatories

Received 1985 January 21; accepted 1985 May 2

ABSTRACT

Nineteen late-type spirals have had their *UBVJHK* colors and CO and H₂O indices measured through an aperture of diameter 6". These data are used to investigate the stellar content of the nuclei of the galaxies.

The overall result of this investigation is that there must be a highly composite stellar population present in the nuclei. The optical light has a significant contribution from young stars with ages less than a few hundred Myr, while the infrared light is dominated by a much older population. These old stars appear to be similar to those in elliptical galaxies although there may be a sizable contribution from luminous M stars such as those found in Magellanic Cloud clusters with ages of a few Gyr.

Numerical analysis of the colors shows that there is no correlation between the *UBV* ones and the *JHK* ones. Thus the star formation rate averaged over the past 100 Myr, which will be the main factor determining the *UBV* colors, must vary considerably from galaxy to galaxy; furthermore, it must be largely uncorrelated with the underlying old stellar population. This old population appears to be similar in all of the galaxies observed.

The photometric data do not permit a significant contribution from old, metal-poor stars at any wavelength, nor do these data permit a significant contribution to the infrared light from luminous carbon stars.

There is evidence for considerable extinction—more than 1.5 mag in A_V —due to material in the immediate vicinity of the Sc nuclei. In many cases this extinction is greater than that which would be inferred from the inclination angle of the galaxy to the line of sight alone.

The $U-V$ and $V-K$ colors of the nuclei of the Sc's are much redder than those of regions somewhat farther out. These color gradients are several times steeper than they are for early-type galaxies. The gradients can be attributed to a radial dependence of the internal reddening and the relative numbers of different types of stars. The latter can arise from a combination of radial gradients in $[Fe/H]$, the recent star formation rate, and a mixture of a disk and a bulge population.

Subject headings: galaxies: nuclei — galaxies: stellar content — stars: formation

I. INTRODUCTION

Since the Milky Way is classified as an early Sc or Sbc spiral galaxy (Hodge 1983), the investigation of the stellar content of the nuclei of other late-type spirals could have relevance to a determination of the stellar population of the nuclear bulge of the Milky Way. The inner few arcseconds of a typical nearby spiral correspond to the inner few degrees of the Milky Way. Most of this region is heavily obscured by dust. Whitford (1978) showed that spectral features in the integrated optical light of Baade's Window at a galactic latitude of $-3^\circ 9'$ are quite similar to those seen in the nuclei of elliptical galaxies. But there are well-documented differences between the nuclei of late-type spirals and ellipticals (e.g., Alloin 1973; Turnrose 1976; O'Connell 1982). Does this mean, then, that if the Milky Way is typical of late-type spirals there is a very strong population gradient in the bulge perpendicular to the plane? Such a gradient could simply be caused by an overlap between two populations with different spatial distributions, e.g., a spheroidal and a disk population. Do Sc's have significantly different nuclear populations than somewhat earlier type galaxies?

Cowley, Crampton, and McClure (1982, hereafter CCM) combined the spectra of five similar late Sc galaxy nuclei and concluded that the summed spectrum could best be modeled by a predominantly old and metal-poor population. Only a

small fraction of the light could come from some combination of B stars, K stars, or metal rich globular clusters. Stars of spectral type A–F are ruled out of their model because the resulting Balmer lines would be too strong. A similar analysis applied to the spectra of a group of somewhat earlier Sc's resulted in similar conclusions, but with a shift toward a larger population of metal-rich globulars. It is worth emphasizing that with the exception of Mg *b*, CCM's analysis is based on line indices to the blue of 4268 Å.

Other analyses of the blue and visual light from spirals have resulted in conclusions quite different from those of CCM. For example, Morgan's (1962) spectroscopic survey showed the Sa–Sc's to have the most mixed stellar population of common galaxies in the Hubble sequence. Detailed quantitative work on spirals, both photometric and spectroscopic, has shown that they consist of mixtures of old and young stars with a range of metallicity. Examples are Searle, Sargent, and Bagnuolo (1973), Turnrose (1976), Heckman (1980), and O'Connell (1982, 1983). While these authors disagree on the details of the mix of old and young stars, none of their models permit any substantial contribution from old, metal-poor stars.

This paper investigates the stellar content of Sc galaxy nuclei based on new small-aperture *UBVJHK*, H₂O, and CO photometry of a sample of 19 southern galaxies. These data are analyzed by a comparison with the integrated colors of star clusters with well-determined stellar populations and with the colors of elliptical galaxies. The cluster and elliptical galaxy data are from earlier papers in this series: Frogel *et al.* (1978,

¹ The Cerro Tololo Inter-American Observatory is operated by the Association of Universities for Research in Astronomy, Inc., under contract with the National Science Foundation.

hereafter Paper I), Aaronson, Frogel, and Persson (1978, hereafter Paper II), and Persson, Frogel, and Aaronson (1979, hereafter Paper III) for elliptical galaxies; Frogel, Persson, and Cohen (1980, hereafter Paper IV) for M31 clusters; Aaronson *et al.* (1978, hereafter ACMM) for Galactic globular clusters; and Persson *et al.* (1983, hereafter Paper V) for Magellanic Cloud clusters.

Infrared data make a valuable addition to the existing optical studies of spiral galaxy nuclei for two main reasons. First, these data are quite sensitive to the presence of the types of stars to be expected in an old population, independent of metallicity. The effects of hot, young stars are suppressed. Second, as was shown in Paper V, clusters of intermediate and young age have stellar populations whose photometric signatures are most obvious in the infrared. These include luminous asymptotic branch giants (both Cs and Ms), and red supergiants. If such stars are present in spiral galaxy nuclei, they should be easily detectable in the infrared.

The approach adopted in this paper is to try to reproduce the continuous energy distribution of late-type spirals from the ultraviolet to the infrared with the energy distributions of objects whose stellar content is relatively well understood. Constraints set on the stellar population by the broad-band colors must be met in any more detailed attempt at modeling these systems. Broader implications of the present results will be addressed elsewhere.

II. THE DATA

a) The Sample

The sample consists primarily of bright Sc galaxies that could be conveniently observed in the optical and infrared during two observing runs devoted to this program. Known Seyferts and strong emission-line galaxies were excluded. All relevant literature for the selected galaxies as compiled by Sandage and Tammann (1981) was checked for remarks about emission lines. Subsequently it was learned that NGC 1637 has weak Seyfert 2/Liner characteristics (Keel 1983), as does NGC 7590 (Phillips 1984). NGC 157 and 6744 also appear to have weak Liner characteristics (Phillips 1984; Keel 1983). Nonetheless, the sample as a whole is characteristic of Sc galaxies with the weakest emission lines. The reader is referred to § IIIb of Turnrose's (1976) study for a more complete description of the emission-line spectra of three of the galaxies in the present investigation—NGC 628, 1084, and 1637.

One objective of this paper is to compare results with CCM. There is, unfortunately, only one galaxy in common to the two samples—NGC 628. CCM's data were obtained with a $3'' \times 10''$ slit which is equivalent in area to a $6''.2$ diameter aperture. Since it is possible that the results can depend strongly on radial distance from the nucleus, Figure 1 compares the distribution—in $\log A/D(0)$ —of the two samples. The median $\log A/D(0)$ of the present samples is only 0.2 dex larger than that of CCM's. Also, the galaxies in the two samples are closely similar in morphological type and emission-line characteristics. Hence, it will be assumed that the present results are directly comparable with those of CCM.

b) Optical Photometry

The *UBV* data were obtained at the f/13 focus of the CTIO 1.5 m reflector. An S20 photomultiplier and standard filter set were used. Transformation of the instrumental magnitudes and colors to the *UBV* system defined by a subset of the highest

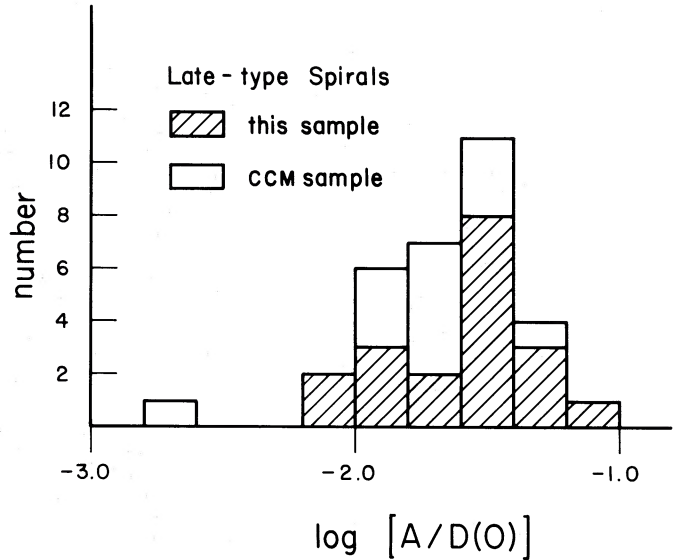


FIG. 1.—The distributions of aperture size relative to galaxy diameter for the present sample and for the CCM sample.

accuracy standards from Landolt (1973) was accomplished in a straightforward manner. First-order extinction corrections were determined empirically. With few exceptions all of the *UBV* data were obtained at $\sec z$ values less than 1.2 to minimize effects of differential refraction. Each galaxy was measured through apertures of diameters $4''.76$ and $7''.21$ to allow interpolation to match up with the infrared measurements. Scans of stars through the apertures showed an essentially flat instrumental response function. Stars close to the galaxies were observed to correct for seeing effects. Sky positions were chosen based on inspection of Palomar or ESO sky survey photographs, and the telescope was offset frequently by computer to the sky position during the course of a measurement.

Final values for colors and magnitudes corrected for all instrumental effects are given in columns (5)–(7) of Table 1. Uncertainties in these values, based on the Poisson statistics of the measurement and the repeatability of the $([\text{object} + \text{sky}] - \text{sky})$ differences, are 0.05 mag or less.

c) Infrared Photometry

Nearly all of the infrared data for the galaxies were obtained in 1983 October with the CTIO 4 m telescope, an f/30 chopping secondary, and the D3 InSb system. Most of the galaxies measured had nuclear condensations visible with the on-axis TV guider. In all cases the centering of the galaxy was checked by peaking up the infrared signal. A few galaxies did not have central condensations visible on the TV with the f/30 chopping secondary. For these the coincidence of the optical and infrared centers could not be verified. Since at the time of observation beam-switching could only be done north-south, those galaxies extended primarily in this direction were not observed. Although an oversimplification, it was assumed that the galaxy light profile in the region of interest resembles that for spheroidal systems. Thus flux in the reference beam was corrected for in a manner identical to that used in Paper I. Computed corrections to the *K* magnitude were between 0.03 and 0.06 mag. The colors need not be corrected. For a few galaxies it was empirically verified that corrections of this size are approximately correct.

TABLE 1
OPTICAL AND INFRARED PHOTOMETRY OF SPIRAL GALAXIES

NGC	TYPE	Z A _v	Log [A/D(0)]	Corrected for Instrumental Effects Only							
				V	U-V	B-V	K	J-K	H-K	H ₂ O	CO
(1)	(2)	(3)	(4)	(5)	(6)	(7)	(8)	(9)	(10)	(11)	(12)
151	SBbc	0.0129	-1.60	15.37	1.79	1.16
		0.0	-1.48	11.21	1.01	0.26	0.08	0.10
			-1.42	14.76	1.76	1.09
				-0.03	-0.03	-0.04	+0.04	-0.06	-0.04	...	+0.06
157	Sc	0.006	-1.69	15.40	1.43	0.95
		0.0	-1.57	11.50	1.02	0.29	0.11	+0.105
			-1.51	14.91	1.36	0.92
				-0.01	-0.01	-0.02	+0.02	-0.03	-0.03	...	+0.02
247	Sc	0.0008	-2.30	16.19	0.36	0.42
		0.0	-2.16	14.11	0.75	0.14
			-2.12	15.80	0.34	0.46
				0.00	0.00	0.00	0.0	0.0	0.0	...	0.0
628	Sc	0.0029	-2.11	15.50	1.14	0.83
		0.03	-1.99	11.95	0.91	0.21	0.11	0.145
			-1.93	14.76	1.37	0.91
				-0.04	-0.02	-0.02	+0.01	-0.01	-0.01	...	+0.01
908	Sc	0.0052	-1.77	15.26	1.28	1.05
		0.0	-1.63	10.85	1.19	0.36	0.16	0.155
			-1.59	14.77	1.37	0.95
				-0.01	-0.01	-0.02	+0.02	-0.03	-0.03	...	+0.015
1084	Sc	0.0049	-1.50	15.17	0.86	0.69
		0.0	-1.38	11.13	1.13	0.34	0.12	0.115
			-1.32	14.46	1.02	0.78
				-0.01	-0.01	-0.01	+0.02	-0.02	-0.02	...	+0.015
1232	Sc	0.0059	-1.98	15.71	1.66	1.11
		0.0	-1.86	11.93	0.93	0.27	0.11	0.11
			-1.80	15.06	1.55	1.03
				-0.01	-0.01	-0.02	+0.02	-0.03	-0.03	...	+0.02
1385	Sc	0.0066	-1.54	15.35	0.00	0.31
		0.0	-1.40	12.25	0.95	0.27	0.08	0.13
			-1.36	14.63	0.16	0.41
				-0.01	-0.01	-0.02	+0.02	-0.03	-0.03	...	+0.02
1448	Sc	0.0035	-1.86	15.89	1.35	0.99
		0.0	-1.72	11.35	1.19	0.37	0.14	0.18
			-1.68	15.11	1.55	1.03
				-0.01	-0.01	-0.01	+0.01	-0.02	-0.02	...	+0.01
1637	SBc	0.0024	-1.61	15.25	1.09	0.86
		0.13	-1.49	11.09	1.09	0.33	0.15	0.14
			-1.43	14.72	1.28	0.94
				-0.13	-0.08	-0.05	0.00	-0.03	-0.02	...	+0.01
1792	Sc	0.0035	-1.63	15.27	1.40	1.05
		0.09	-1.51	10.94	1.18	0.37	0.16	0.125
			-1.45	14.68	1.40	0.94
				-0.10	-0.06	-0.04	0.00	-0.03	-0.03	...	+0.01
2090	Sc	0.0025	-1.68	15.25	1.28	0.84
		0.15	-1.54	11.79	0.89	0.23	0.10	0.12
			-1.50	14.52	1.37	0.92
				-0.15	-0.09	-0.06	0.00	-0.03	-0.02	...	+0.01
2207	Sc	0.0086	-1.69	14.47	1.68	1.14
		0.32	-1.57	10.45	0.99	0.27	0.11	0.12
			-1.51	14.01	1.80	1.12
				-0.34	-0.20	-0.13	0.00	-0.09	-0.05	...	+0.035
6744	SBc	0.0022	-2.25	14.52	1.81	1.17
		0.17	-2.11	10.52	0.91	0.23	0.08	0.135
			-2.07	13.86	1.71	1.10
				-0.17	-0.10	-0.06	-0.01	-0.04	-0.02	...	+0.005

TABLE 1—Continued

NGC (1)	TYPE (2)	Z A_V (3)	Log $[A/D(0)]$ (4)	Corrected for Instrumental Effects Only							
				V (5)	$U-V$ (6)	$B-V$ (7)	K (8)	$J-K$ (9)	$H-K$ (10)	H_2O (11)	CO (12)
7316	--	0.0193	12.37	0.97	0.33	...	0.07
		0.11	+0.05	-0.10	-0.08	...	+0.10
7412	Sc	0.0056	-1.67	16.09	0.75	0.71
		0.0	-1.53	12.60	0.92	0.26
			-1.49	15.52	1.01	0.84
7418	Sc	0.0048	-1.60	15.88	0.46	0.56
		0.0	-1.46	12.21	1.00	0.31	0.11	0.150
			-1.42	15.56	0.58	0.66
7590	Sc	0.0050	-1.44	14.76	1.58	1.13
		0.0	-1.30	10.78	0.99	0.26	0.11	0.135
			-1.26	14.28	1.48	1.04
7793	Sd	0.0008	-2.03	14.88	0.34	0.46
		0.0	-1.89	12.26	0.75	0.19	0.05	0.13
			-1.85	14.55	0.40	0.48
				0.00	0.00	0.00	0.00	0.00	0.00	...	0.00

NOTE.—The two UBV entries for each galaxy are based on measurements made through apertures of diameter $4''.76$ and $7''.21$. The infrared data were obtained through either $6''.3$ or $6''.6$ diameter apertures.

The silicon field lens in D3 used for the first set of infrared observations resulted in strongly wavelength dependent beam profiles. This effect was corrected for by determining the radial response function in the aperture by scans of a star and convolving the response function with a standard galaxy profile. Again, this follows the procedure of Paper I. Typical corrections to K , $J-K$, and $H-K$ are 0.02, 0.05, and 0.02 mag. A second set of observations, with a new field lens will be described below.

Columns (8)–(12) of Table 1 give the infrared magnitudes, colors, and narrow-band indices, corrected for all instrumental effects. These values are on the CIT/CTIO photometric system defined by the standards of Elias *et al.* (1982). Uncertainties in these values, excluding those which might arise from beam profile and chopper throw corrections, are 0.03 mag or less for the broad-band data and 0.02 mag or less for the narrow-band indices. These indices have relatively small uncertainties because of the essentially identical beam profiles of the filters used to determine them.

In 1983 November multiaperture infrared observations were made for five of the galaxies in Table 1. The five were selected because of their particularly red (or blue) colors and a desire to test for radial dependence of these colors. These data were obtained with the same instrumental set-up as for the infrared data in Table 1 except that different beam separations were used and, more importantly, a new doublet field lens made of BaF and LiF was installed in D3. This design eliminates wavelength-dependent beam profiles.

Over the range of aperture sizes usable with D3 on the 4 m telescope, the beam profiles at J , H , and K with the new lens are quite rectangular and nearly independent of wavelength. The largest correction which needed to be applied to the $J-K$ and $H-K$ colors was found to be 0.01 mag. These supplemental data, corrected for instrumental effects in the same manner as the Table 1 data, are the observed values given in Table 2. Reddening- and redshift-corrected values are also given.

Data obtained with the two field lenses were compared by interpolating between the values in Table 2 to match the $\log A/D(0)$ values in Table 1. The mean differences and dispersions are given in Table 3. The two sets of $H-K$ values are essentially identical. The small *dispersions* in the $J-K$ and $H-K$ colors are consistent with the small photometric uncertainties. The relatively large dispersion in the two sets of K magnitudes can be understood as arising from small errors in the setting of the iris diaphragm used to define the focal plane aperture and uncertainties in the beam separation and beam profile corrections. The apparently significant systematic difference in the $J-K$ color most likely arises from a systematic error in the profile corrections applied for the old field lens

TABLE 2
MULTIAPERTURE DATA

NGC	Log $[A/D(0)]$	OBSERVED VALUES			CORRECTED VALUES		
		K	$J-K$	$H-K$	K_0	$(J-K)_0$	$(H-K)_0$
151....	-1.77	12.10	1.04	0.28	12.14	0.98	0.24
	-1.45	11.12	0.99	0.27	11.16	0.93	0.23
	-1.25	10.63	0.97	0.27	10.67	0.91	0.23
908....	-1.94	11.70	1.13	0.37	11.72	1.10	0.34
	-1.62	10.79	1.17	0.37	10.81	1.14	0.34
	-1.42	10.38	1.16	0.36	10.40	1.13	0.33
1084....	-1.67	12.01	1.15	0.37	12.03	1.13	0.35
	-1.35	11.03	1.09	0.35	11.05	1.07	0.33
	-1.15	10.54	1.03	0.30	10.56	1.01	0.28
1385....	-1.51	12.54	0.91	0.25	12.56	0.88	0.22
	-1.21	11.39	0.90	0.25	11.41	0.87	0.22
1792....	-1.78	11.77	1.12	0.36	11.77	1.09	0.33
	-1.46	10.81	1.15	0.35	10.81	1.12	0.32
	-1.28	10.33	1.14	0.34	10.33	1.11	0.31
7590....	-1.61	11.47	0.97	0.26	11.49	0.95	0.24
	-1.29	10.75	0.96	0.26	10.77	0.94	0.24
	-1.09	10.36	0.95	0.25	10.38	0.93	0.23

TABLE 3
MEAN DIFFERENCES AND DISPERSIONS
(1982 November) – (1983 October)

Parameter	ΔK	$\Delta(J-K)$	$\Delta(H-K)$
Mean ^a	-0.03	-0.03	0.00
Dispersion	0.05	0.01	0.01

^a Based on six galaxies.

used for the 1983 October observations. The conclusions of this paper are not affected by this difference; hence, no attempt was made to correct for it.

d) Reddening and Redshift Corrections

Galactic reddening was dealt with in a manner similar to that employed in Paper III. The absorption-free polar cap model (Sandage 1973) yields values of $A_V = 0.1 (\csc b - 1)$ for $|b| < 50^\circ$. Color excesses are as given in the Appendix of Cohen *et al.* (1981) with the addition that $E(U-V) = 1.71 \times E(B-V)$. The color dependence of the ratio of total to selective absorption is as given by Olson (1975).

Infrared K -corrections, which are nearly linear with z , are from Paper I. They are $-4.0z$, $-3.5z$, and $+3.3z$ for $J-K$, $H-K$, and K , respectively. Optical K -corrections from Whitford (1971) and Sandage (1972) are given by $-2z$, $-3z$, and $-2z$ for $U-V$, $B-V$, and V , respectively. These corrections are based on observations of elliptical galaxies and, strictly speaking, should not be used for the bluer galaxies in the present sample. However, their redshifts are small enough that no significant errors are introduced by the procedure followed.

The last line for each galaxy in Table 1 gives the corrections to be applied to the data for Galactic reddening and redshift.

e) Combined Optical and Infrared Data

Interpolation between the UBV data in Table 1 yields colors and magnitudes appropriate to the $\log [A/D(0)]$ values of the infrared data. The indicated corrections were applied and final colors and magnitudes obtained. These values are given in Table 4.

Sandage and Tammann (1981) give extinction values for all but one of the galaxies in Table 4. These values are a function of inclination angle only. They are given in the third column of Table 4. Their effect on the interpretation of the data will be discussed below.

III. RADIAL COLOR GRADIENTS

All of the galaxies observed for the present program have been observed previously in the optical and/or the infrared but with apertures substantially larger than those employed here. These previously published data have been combined with data from Table 1 to form the color differences in Table 5. Small corrections were applied to the published infrared colors to place them on the CTIO/CIT system. The color differences listed in Table 5 show that although some of the spirals tend to get bluer in $U-V$ with decreasing aperture size, the majority get redder toward the nucleus, i.e., most of the values in the penultimate column of Table 5 are positive. The $J-K$ and $V-K$ colors are also markedly redder in small apertures than in large ones.

Normalized $U-V$ gradients [change per unit change in $\log A/D(0)$] do not show a great deal of scatter: for 11 of the 18 galaxies the normalized gradient lies between 0.2 and 0.6. Five galaxies have normalized $U-V$ gradients less than 0.2, while only two have gradients greater than 0.6. The four galaxies with negative $U-V$ gradients, NGC 247, 1385, 7418, and 7793, are also the four bluest in $(U-V)_0$ as may be seen from Table 4. (The nucleus of NGC 7793 has been studied by Diaz *et al.*

TABLE 4
GALAXY DATA CORRECTED FOR GALACTIC REDDENING AND REDSHIFT

NGC (1)	Type (2)	A_i (3)	$M_{B_T}^{0,i}$ (4)	$\log A/D(0)$ (5)	$(U-V)_0$ (6)	$(B-V)_0$ (7)	$(V-K)_0$ (8)	K_0 (9)	$(J-K)_0$ (10)	$(H-K)_0$ (11)	H ₂ O (12)	CO (13)
151.....	SBbc	0.54	-22.70	-1.48	1.74	1.07	3.68	11.25	0.95	0.22	0.08	0.16
157.....	Sc	0.43	-22.19	-1.57	1.37	0.91	3.53	11.52	0.99	0.26	0.11	0.125
247.....	Sc	0.63	-18.62	-2.16	0.34	0.45	1.77	14.11	0.75	0.14
628.....	Sc	0.31	-21.75	-1.99	1.27	0.87	3.00	11.96	0.90	0.20	0.11	0.155
908.....	Sc	0.54	-22.15	-1.63	1.34	0.94	3.99	10.87	1.16	0.33	0.16	0.17
1084.....	Sc	0.52	-21.62	-1.38	0.96	0.74	3.53	11.15	1.11	0.32	0.12	0.13
1232.....	Sc	0.32	-22.57	-1.86	1.57	1.04	3.31	11.95	0.90	0.24	0.11	0.13
1385.....	Sc	0.44	-21.77	-1.40	0.11	0.37	2.50	12.27	0.92	0.24	0.08	0.15
1448.....	Sc	0.85	-21.14	-1.72	1.50	1.01	3.91	11.36	1.17	0.35	0.14	0.19
1637.....	SBc	0.33	-19.72	-1.49	1.14	0.86	3.66	11.09	1.06	0.31	0.15	0.15
1792.....	Sc	0.53	-21.39	-1.51	1.34	0.94	3.83	10.94	1.15	0.34	0.16	0.135
2090.....	Sc	0.53	-19.72	-1.54	1.26	0.85	2.73	11.79	0.86	0.21	0.10	0.13
2207.....	Sc	0.43	-22.97	-1.57	1.57	1.00	3.37	10.45	0.90	0.22	0.11	0.155
6744.....	Sbc	0.44	-21.98	-2.11	1.63	1.05	3.31	10.51	0.87	0.21	0.08	0.14
7316.....	S	0.36	...	-1.07	12.42	0.87	0.25	...	0.17
7412.....	Sc	0.38	-20.98	-1.53	0.94	0.80	3.01	12.62	0.89	0.23
7418.....	Sc	0.35	-20.66	-1.46	0.55	0.62	3.39	12.23	0.98	0.29	0.11	0.165
7590.....	Sc	0.61	-20.78	-1.30	1.49	1.04	3.57	10.80	0.97	0.24	0.11	0.15
7793.....	Sd	0.40	-18.85	-1.89	0.39	0.47	2.36	12.26	0.75	0.19	0.05	0.13

NOTE.—Cols. (2)–(4) are from Sandage and Tammann 1981 except for NGC 7316. The types have been abbreviated somewhat. A_i is the total internal extinction from col. (14) of Sandage and Tammann. The present data have not been corrected for this extinction except for the absolute B magnitudes, $M_{B_T}^{0,i}$, which are taken directly from Sandage and Tammann. The UBV values in this table are obtained by interpolation from the data of Table 1 with the indicated corrections applied. The infrared data are those of Table 1 with the corrections applied.

TABLE 5
TEST FOR COLOR GRADIENTS
 $\Delta[(\text{This Paper}) - (\text{Other References})]$

NGC	$\log Ap$	K	$J-K$	$H-K$	$V-K$	V	$U-V$	Notes
151.....	-0.64	1.40	+0.04	-0.01	0.37	...	+0.20	1
157.....	-1.22	3.48	+0.09	+0.01	0.54	...	+0.68	1
247.....	-1.39	4.89	-0.29	2
628.....	-0.64	2.25	+0.06	-0.03	+0.21	3
908.....	-0.99	2.90	+0.51	2
1084.....	-0.64	1.80	+0.17	+0.06	0.28	...	+0.27	1, 4
1232.....	-0.64	1.61	+0.06	+0.07	0.23	...	+0.32	1, 5
1385.....	-0.99	2.98	-0.16	2
1448.....	-1.31	3.87	+0.58	2
1637.....	-0.64	1.15	+0.13	+0.06	0.36	...	+0.05	1
1792.....	-1.41	4.54	+0.60	6
2090.....	-0.99	3.00	+0.24	2
2207.....	-0.70	1.31	+0.43	2
6744.....	-1.00	2.21	+0.08	+0.04	...	1.66	+0.32	7
7316.....	-0.76	1.67	+0.04	+0.03	1
7412.....	-1.20	3.83	+0.32	8
7418.....	-0.65	1.69	-0.29	8
7590.....	-0.26	0.68	+0.12	9
7793.....	-0.65	1.77	+0.67	8
	-0.50	1.26	-0.21	10
	-0.99	3.04	-0.21	2
Normalized color means ^a			+0.12	+0.04	+0.48	...	+0.35	

NOTES.—(1) Infrared and optical photometry from Aaronson 1977. (2) Optical photometry is from de Vaucouleurs and de Vaucouleurs 1972. (3) Infrared photometry from Aaronson 1977. Optical photometry from de Vaucouleurs, de Vaucouleurs, and Corwin 1978 corresponds to $\Delta \log Ap = -0.70$. (4) For this galaxy the Δ 's for the H_2O and CO indices are +0.015 and +0.03, respectively, from Aaronson's 1977 data. (5) For $V-K$ and the optical photometry $\Delta \log Ap = 1.01$. (6) Optical photometry from de Vaucouleurs, de Vaucouleurs, and Corwin 1978. (7) Infrared photometry from Aaronson 1977. The optical photometry is from Alcaïno 1974, and for it $\Delta \log Ap = +0.50$. (8) Optical photometry from Shobbrook 1966. (9) Optical photometry from Glass 1973. (10) Optical photometry from Alcaïno 1974.

^a The means are normalized to $\Delta(\log Ap) = -1.0$.

1982.) Three of these four, NGC 7418 being the exception, are also the bluest in $(V-K)_0$. There is no particular correlation between red nuclear colors, either $(U-V)_0$ or $(V-K)_0$, and large positive gradients.

It is interesting to compare these gradients for late-type spirals with those elliptical galaxies. The normalized $J-K$ and $H-K$ gradients for spirals (last line of Table 5) are identical to the values found for a large sample of Es and S0's (the right-hand side of Table 3 in Paper I). The gradients in $U-V$ and $V-K$ for spirals, on the other hand, are several times greater than typical values for early-type galaxies which are 0.14 and 0.11, respectively (Paper I; de Vaucouleurs and de Vaucouleurs 1972).²

In contrast to the individual gradient values, the *ratios* of the gradients in spirals are quite similar to the *slopes* in color-color diagrams for the integrated colors of early-type galaxies. Values of these quantities are given in Table 6. [The $(J-K)/(U-V)$ value for Es and S0's is somewhat different than that given in Table 8 of Paper I because of the inclusion of data from Paper III.] Both values of $(V-K)/(U-V)$ in Table 6 here are significantly less than the reddening ratio of 1.72 and probably reflect some combination of stellar population and metallicity gradients.

² It should be noted that the small-aperture photometry of spirals presented here corresponds to values of $\log A/D(0)$ several tenths of a dex more negative than most of the smallest aperture photometry available for ellipticals. Also it is not obvious how appropriate this type of comparison is since the $D(0)$ values for the spirals refer mainly to the disks rather than their central bulges.

IV. STATISTICAL ANALYSIS OF THE COLORS

To bring some order to the large number of colors and indices measured for the spirals, two lines of approach will be followed. First correlations will be looked for between the observed quantities. Then a principal component analysis will be performed to determine how many independent variables there really are.

a) Correlation Coefficients

For each galaxy we have five broad-band colors, the CO and H_2O indices, and the absolute B magnitudes. These quantities are all given in Table 4. Table 7A gives the mean, the standard

TABLE 6
RATIOS OF COLOR GRADIENTS^a

Type of Object	$\frac{J-K}{U-V}$	$\frac{V-K}{U-V}$
Late-type spirals	0.33	1.28
Es, S0's globulars	0.3 ^b	1.3 ^b
Reddening ratios	0.32	1.72

^a Based only on those galaxies from Table 5 having values for each of the two colors in a given ratio. These values were first normalized.

^b These values are ratios of color variations *between* individual galaxies and clusters as determined by an eyefit to the data in Figs. 1 and 2 of Frogel, Persson, and Cohen 1980.

TABLE 7A
VARIABLES USED IN THE ANALYSIS

Variable	Mean	Standard Deviation	Error
$M(B)_0$	-21.198	1.276	0.30
$(J-K)_0$	0.960	0.128	0.02
$(H-K)_0$	0.252	0.059	0.02
H_2O	0.099	0.046	0.02
CO	0.131	0.051	0.02
$(V-K)_0$	3.247	0.590	0.10
$(U-V)_0$	1.139	0.489	0.05
$(B-V)_0$	0.836	0.221	0.05

TABLE 7B
THE CORRELATION COEFFICIENTS (COVARIANCES)

Variable	$M(B)_0$	$(J-K)_0$	$(H-K)_0$	H_2O	CO	$(V-K)_0$	$(U-V)_0$	$(B-V)_0$
$M(B)_0$	1.000							
$(J-K)_0$	-0.365	1.000						
$(H-K)_0$	-0.261	0.960	1.000					
H_2O	-0.379	0.799	0.799	1.000				
CO	-0.418	0.506	0.501	0.805	1.000			
$(V-K)_0$	-0.587	0.847	0.798	0.781	0.608	1.000		
$(U-V)_0$	-0.597	0.362	0.233	0.473	0.384	0.711	1.000	
$(B-V)_0$	-0.592	0.418	0.301	0.494	0.379	0.763	0.990	1.000

TABLE 7C
PROBABILITY OF SIGNIFICANCE FOR CORRELATION COEFFICIENTS

Variable	$M(B)_0$	$(J-K)_0$	$(H-K)_0$	H_2O	CO	$(V-K)_0$	$(U-V)_0$	$(B-V)_0$
$M(B)_0$	1.000							
$(J-K)_0$	0.864	1.000						
$(H-K)_0$	0.705	1.000	1.000					
H_2O	0.879	1.000	1.000	1.000				
CO	0.916	0.968	0.966	1.000	1.000			
$(V-K)_0$	0.990	1.000	1.000	1.000	0.993	1.000		
$(U-V)_0$	0.991	0.860	0.648	0.952	0.885	0.999	1.000	
$(B-V)_0$	0.990	0.916	0.776	0.963	0.879	1.000	1.000	1.000

TABLE 7D
THE EIGENVALUES

Eigenvectors (1)	Eigenvalue (2)	Percent Variation (3)	Variation due to Error (4)	Ratio (5)	Probability (6)
V1	0.005	0.060	0.003	1.77	0.87
V2	0.023	0.288	0.007	3.49	0.99
V3	0.038	0.478	0.017	2.28	0.95
V4	0.111	1.388	0.109	1.02	0.51
V5	0.515	6.433	0.057	9.04	1.00
V6	0.678	8.471	0.123	5.50	1.00
V7	1.542	19.274	0.050	30.61	1.00
V8	5.089	63.608	0.079	64.64	1.00

TABLE 7E
THE EIGENVECTORS

Variable	V1	V2	V3	V4	V5	V6	V7	V8
$M(B)_0$	0.019	-0.067	-0.027	0.155	-0.849	0.220	-0.348	0.283
$(J-K)_0$	-0.093	-0.384	-0.675	-0.076	0.136	0.332	-0.346	-0.375
$(H-K)_0$	0.052	0.734	0.145	0.134	0.107	0.298	-0.446	-0.347
H_2O	-0.003	-0.124	0.327	-0.740	-0.231	-0.256	-0.245	-0.389
CO	-0.049	0.080	-0.242	0.418	-0.174	-0.778	-0.141	-0.320
$(V-K)_0$	0.170	-0.489	0.537	0.470	0.020	0.196	0.000	-0.428
$(U-V)_0$	0.655	0.172	-0.261	-0.092	-0.294	0.117	0.508	-0.326
$(B-V)_0$	0.727	0.136	0.002	0.026	-0.279	0.190	0.472	-0.340

deviation, the variance, and the assigned error for each of these quantities. For ease in later computation, all of the variables are normalized so as to have 0.0 mean and unit standard deviation (cf. Faber 1973; Deeming 1964). Following Bevington (1968), the correlation coefficients for all of the variables are computed and given in Table 7B. Because of the normalization, the correlation coefficients are equal to the covariances. The probability of significance of the correlation coefficients are computed with a Student t -test and given in Table 7C.

There are 14 pairs of variables whose correlation coefficients are significant at the 99% level or greater. These are underlined in Tables 7B and 7C. These 14 pairs fall into three well-separated groups. In the first group, with correlation coefficients greater than 0.95 there are, not surprisingly, $[(J-K), (H-K)]_0$ and $[(U-V), (B-V)]_0$. In the second group with correlation coefficients between 0.7 and 0.85 are both $(J-K)_0$ and $(H-K)_0$ with each of H_2O and $(V-K)_0$, both $(U-V)_0$ and $(B-V)_0$ with $(V-K)_0$, and H_2O with CO and $(V-K)_0$. In the third group with correlation coefficients between 0.58 and 0.61 are $M(B)_0$ with $(U-V)_0$, $(B-V)_0$, and $(V-K)_0$, and CO with $(V-K)_0$.

The advantage of identifying the correlated quantities is that the form of the correlation can then be compared with that for other classes of objects. Such a comparison will be the basis of the approach to the analysis of the nuclei in § V. Also, it is apparent that if the relationship of $U-V$ (or $J-K$) to the other parameters is investigated, it is not necessary to investigate that of $B-V$ (or $H-K$) as well. Thus the number of color-color plots worth inspecting is reduced considerably.

It is notable that there is *not* a relatively significant correlation between the optical broad-band colors $U-V$, and $B-V$, and the purely infrared ones, $J-K$, $H-K$. Such correlations are strongly present for globular clusters and early type galaxies (Papers I and IV). Also, there is no significant correlation between the optical colors and the H_2O and CO indices. These results suggest a decoupling between the stars primarily responsible for the blue light and those for the infrared light.

The effect of eliminating from the sample the four galaxies with the bluest UBV colors, NGC 247, 1385, 7418, and 7793 (cf. § III), was investigated. The two main results are as follows: (1) the correlations of all colors with $M(B)$ becomes insignificant; and (2) the probability of significance of the $U-V$, $V-K$ correlation drops to 60%. This latter result is particularly surprising in view of the tight, well-defined correlation between these quantities for elliptical galaxies and globular clusters (Papers I and IV; ACMM). It appears to be due not to a small color range for the remaining 14 galaxies, but rather to their large dispersion in these two colors. That such a dispersion exists is evident even in Aaronson's (1978) smaller sample. This lack of correlation is connected with the lack of correlation between the pure optical and pure infrared colors just noted.

A second test was to repeat the calculations for Tables 7A–7C after eliminating, at random, one-third of the galaxies from the sample. Again, evidence for a correlation between $M(B)_0$ and any color evaporated. Also, the probability of significance for the correlation between $V-K$ and $U-V$ dropped to 95%.

b) Principal Component Analysis

We are dealing with eight photometric indices and wish to investigate the space of minimum dimensionality required to fully describe the Sc galaxy nuclei and what the effect of obser-

vational errors are upon the result. Faber (1973) and Deeming (1964) have described in detail the method of principal component analysis as applied in an astronomical setting. For the present case the normalized values of the eight variables in Table 7A were used for the analysis. Table 7D lists the eigenvalues for the solution (col. [2]); the percent of the total variation contained in each eigenvalue (col. [3]); the amount of the variation due to the assigned errors of Table 7A (col. [4]); the ratio of column (2) to column (4) (col. [5]); and, finally, the probability for the confidence level that the ratio is greater than 1.0 calculated by assuming that the ratio follows the F distribution with $N - 1$ degrees of freedom (col. [6]) (Deeming 1964). Clearly, the last four eigenvectors have significantly greater variation than that due to errors alone at the 0.5% confidence level. These four eigenvectors account for 98% of the total variation.

The eigenvectors corresponding to the eigenvalues of Table 7D are given in Table 7E. V8, which accounts for 63% of the total variation, is an expression of the usual relationship for galaxies which finds all optical and infrared broad-band colors positively correlated with one another and with luminosity. V7, which accounts for 19% of the variation, arises from the significant negative correlation between the pure infrared colors and the pure optical ones. V5 and V6 account for 15% of the total variation. V5, which is primarily a function of $M(B)$, reflects the result from the previous section that the correlation between $M(B)$ and *any* color is relatively weak. Similarly, V6 appears to be due to an independent variation of the CO index. This could be caused by a shift in one component of the stellar population such as is seen in the Magellanic Clouds when one goes from young, supergiant-dominated clusters to older clusters dominated by luminous asymptotic giant branch stars (Paper V).³

V. THE STELLAR CONTENT OF THE SC GALAXY NUCLEI: A COMPARISON WITH STAR CLUSTERS AND ELLIPTICAL GALAXIES

The use of flux ratio diagrams rather than the color-color plots in interpreting the light from composite stellar systems has been explained by Rabin (1980). Such diagrams have been used in Paper V to examine the stellar makeup of Magellanic Cloud clusters. In them the ratio of two fluxes are plotted on a linear scale. One wavelength is chosen as a common denominator for both axes. The advantage of this approach is that a two-component system lies on the straight line segment joining the individual components. The distance to each of the components is inversely proportional to the contribution of each to the flux at the wavelength which is the common denominator (Rabin 1980). Additional components are added in an obvious fashion. In such plots, though, reddening vectors are curved. The effect on a point of a given amount of reddening depends on the location of the point on the diagram.

³ Faber (1973) has cautioned that the stability of a solution such as that in Tables 7D and 7E should be tested against various subsets of the data and against the effect of the observational uncertainties. The two tests described in the previous section were repeated. In both cases there were still four significant eigenvectors, although their components were somewhat different, and together they accounted for somewhat less of the total variation. Other tests included the following: (1) substitution of $J-H$ and $U-B$ for $J-K$ and $U-V$, respectively; (2) elimination of $B-V$ and $H-K$ as variables; (3) increasing the UBV and JHK color errors to 0.10 mag. In all cases the results were the same as those obtained in the tests that simply reduced the sample size.

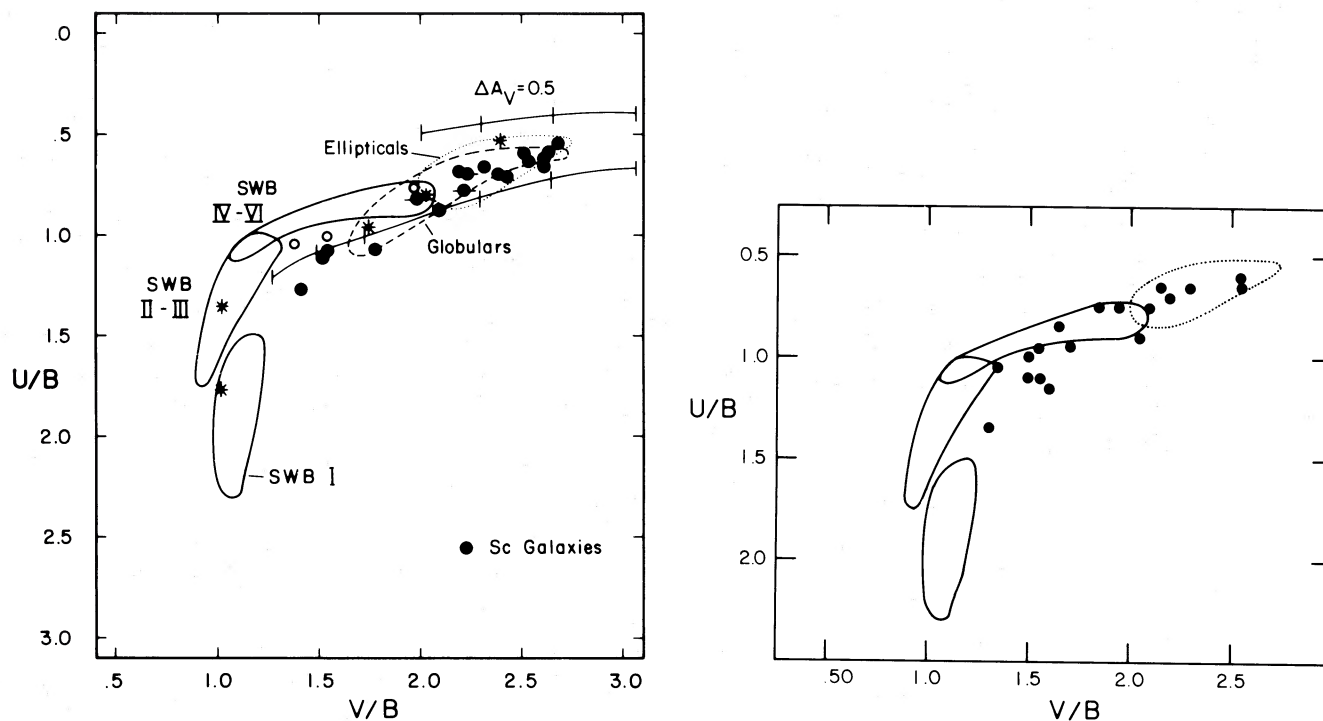


FIG. 2.—A UBV flux ratio plot. Regions occupied by star clusters of different types and by early-type galaxies are shown. Metal-poor globular clusters will always occupy the blue end of the globular sequence. The asterisks denote the locations of the five representative objects from Table 8A. NGC 2173 is at the extreme right of the SWB IV-VI area. The Sc galaxy data are based on the colors in Table 4. Points with short horizontal lines through them are the three galaxies in common with Turnrose's (1976) study. The open circles are these three galaxies dereddened with the A_V values predicted by Turnrose. The two extinction vectors are marked at 0.5 mag intervals. The right-hand panel shows the effect of dereddening the Sc galaxy nuclei by amounts given by assuming that all of their $J-H$ colors are identically equal to 0.65.

Figures 2-6 allow a simple examination of the principal contributions to the flux in Sc nuclei at B , V , H , and K . These particular relationships were chosen with the results of § IV as a guide. The quantities plotted are $10^{0.4 \times \text{color}}$, where "color" is from Table 4 with the appropriate sign. The multiplicative constant needed to convert these quantities to absolute fluxes has not been included.

Magellanic Cloud clusters are divided into three groups according to Searle, Wilkinson, and Bagnuolo (1980, hereafter SWB) type: SWB I's have infrared colors dominated by red supergiants; SWB II-III's have luminous M-type asymptotic giant branch (AGB) stars and ages on the order of 0.1 Gyr. The infrared colors of SWB IV-VI clusters are for the most part dominated by luminous AGB carbon stars with a substantial contribution from AGB M stars. Typical ages are a few Gyr. Reddening-corrected colors for the Cloud clusters are from Paper V supplemented with additional UBV data from the compilation of van den Bergh (1981).

Data for M31 globular clusters in Figures 2-6 are from Paper IV supplemented by UBV colors from van den Bergh (1969). The majority of the data points are more tightly grouped than is indicated by the areas delineated. The location of galactic globular clusters (ACMM) overlaps those of the M31 ones. The globular cluster boundary in Figure 6 is based on the ACMM data because of the small sample of M31 clusters with CO indices.

The E/S0 galaxy data are from Papers I, III, and IV. Again, the majority of data points are clustered in areas considerably smaller than those delineated in the figures. Two reddening vectors are shown on each figure with tick marks indicating either 0.5 or 1.0 mag increments in A_V . Color excess ratios

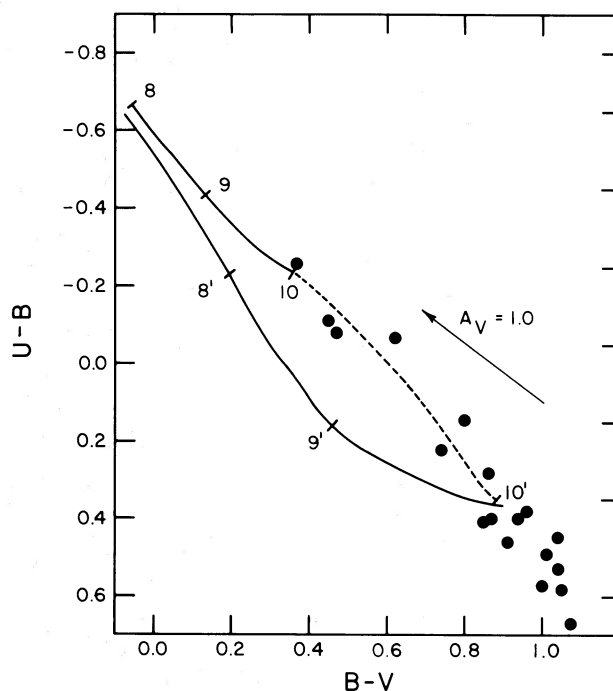


FIG. 3.—A color-color plot with model predicted colors from Searle, Sargent, and Bagnuolo (1973). The numbers are the exponents of the models' ages in years. The primed ages are of models with no star formation since birth, while the unprimed ones are of models with continuous star formation since birth. The dashed line is a sequence of models of the same age but with secularly declining rates of star formation.

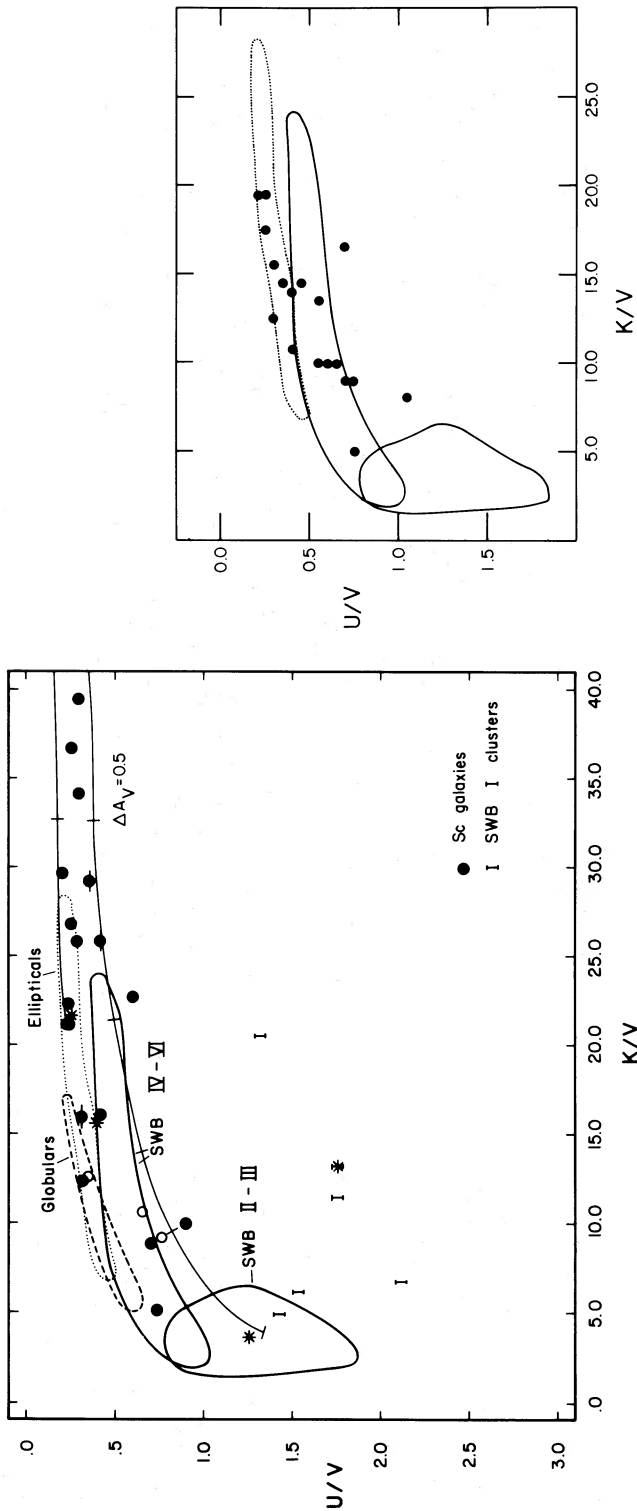


FIG. 4.—A UV/K flux ratio plot. Symbols, etc. are similar to those in Fig. 2 except that the SWB I clusters are shown individually and the MPG asterisk from Table 8A is not shown. The right-hand panel again shows the effect on the Sc nuclei colors of the assumption that all need to be dereddened by an amount which will make their intrinsic $J-H$ colors identically equal to 0.65.

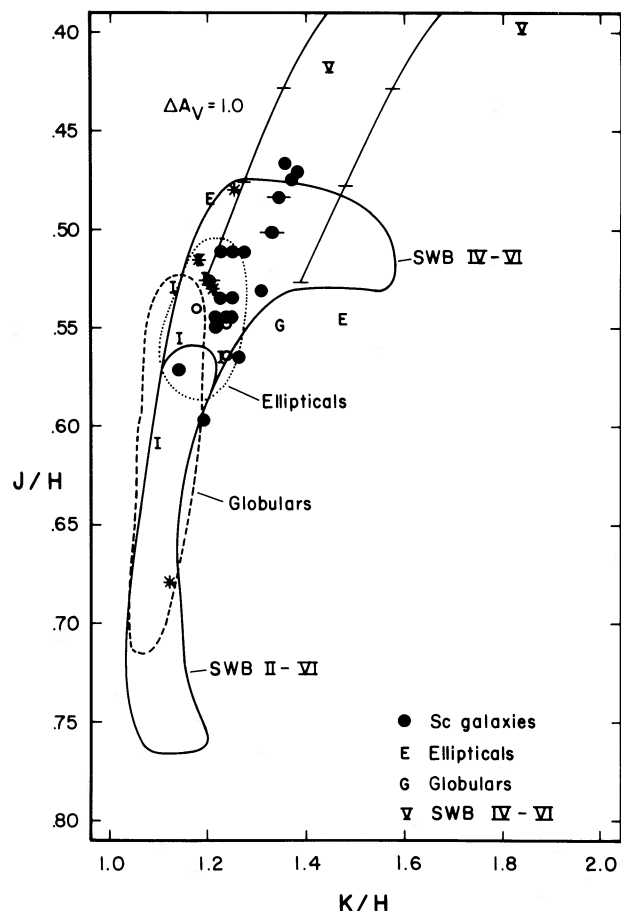


FIG. 5.—Same as Fig. 4 except that intervals of 1.0 mag are now indicated along the reddening vectors. The lower part of the distribution of SWB IV–VI clusters completely overlaps that for the SWB II–III clusters. Some outlying points of the various distributions are shown explicitly. In order of increasing J/H , the asterisks are for NGC 2173, 1805, 4472, and 1854.

intermediate to those for an A0 and an M star (Cohen *et al.* 1981) were used.

a) The Colors: General Trends

i) The Pure Infrared Colors

The relative contributions from star clusters and elliptical galaxy-like systems to the light of Sc nuclei at H and K can be estimated from Figures 5 and 6. The special usefulness of these two figures is that there is little overlap between elliptical galaxies and globular clusters; the SWB IV–VI clusters are clearly separated from the other stellar systems; and in Figure 6 a reddening vector is nearly perpendicular to the cluster sequences rather than parallel to them.

Both Figures 5 and 6 show that a stellar population such as is found in a metal-poor globular cluster cannot contribute significantly to the infrared light of Sc nuclei (as will be shown in § Vd, this effectively rules out any contribution of a metal-poor globular cluster to the B light as well). Neither is there a significant contribution from the extreme SWB IV–VI clusters, i.e., those whose IR light is strongly dominated by carbon stars such as NGC 2009, 2108, and 2231. Such clusters have large values of K/H and of $2.36/K$. Finally, Figure 6 shows that the principal contribution to the K light cannot be reddened globular cluster light of any metallicity.

ii) The UBV Colors

The UBV colors are also inconsistent with CCM's conclusion that the blue light of Sc nuclei is dominated by an old and metal-poor population. As may be seen from Figure 2a most of the Sc nuclei in the present study have UBV flux ratios which closely match those of E/S0 galaxies or globular clusters of intermediate to high metallicity. UBV colors alone cannot readily distinguish between the two groups of objects.

There are three Sc nuclei that lie to the blue of the globular cluster sequence—NGC 247, 1385, and 7793. Even if these three nuclei have no internal absorption, Figure 2a shows that a significant fraction—perhaps more than half—of their B light must come from stars similar to those found in SWB II–III clusters, i.e., with an age comparable to or less than 100 Myr. Again, this result is in strong contradiction to that of CCM. For NGC 7793 Diaz *et al.* (1982) similarly concluded that the blue-violet spectrum is dominated by A or early F stars, not by a mixture of globular cluster-like populations.

Searle, Sargent, and Bagnuolo (1973) calculated UBV colors for simple galaxy models. These calculated colors successfully reproduced integrated colors of open clusters of a variety of ages. Searle *et al.* then showed that the sequence of model colors closely reproduced the integrated colors of late-type galaxies as well. Figure 3 shows that one-third of the present sample of nuclear colors lies along the 10–10' model track. This is the line connecting galaxies which are 10^{10} yr old and have had no star formation since birth (10') and those that are 10^{10} yr old but have had uniform star formation over the time period (10). Between them lie the models with secularly declining rates of star formation. Unless one is prepared to argue (cf. Heckman 1980) that the color sequence for elliptical galaxies arises from continuous star formation over their lifetimes, none of the sequences in Figure 2a overlap the 10'–10 line in Figure 3. Unlike the sample of Searle *et al.*, though, $\frac{2}{3}$ of the present one lies to the red of the 10' point. As the reddening vector shows, dereddening the galaxies by a few tenths will put some of them close to the 8'9'10' track which represents galaxies of age 10^8 – 10^{10} yr. Searle *et al.* argued that such galaxies are at present undergoing a very active period of star formation rather than that they are truly young galaxies. As will be seen, the infrared data are consistent with this view. A period of active star formation is reflected in Figure 2 which, as was noted above, shows that for some of the galaxies the B light contains a significant contribution from young stars of the type found in SWB II–III clusters.

Larson and Tinsley (1978) refined the models of Searle *et al.* somewhat. Their calculations show that for bursts of star formation of a given duration but of various ages, there should be a large scatter in $U-B$ color at a given $B-V$. The small scatter shown by the points in Figures 2a and 3 suggests that if bursts are important in these Sc nuclei, they occur with a frequency of once every few times 10^8 yr. This is consistent with the presence of SWB II–III clusters since their ages are (5×10^7) – (5×10^8) yr (Cohen 1982). Recall, though, that for inclusion in the present study, a galaxy had to have little or no nuclear activity. Any galaxy with a very recent period of active star formation would probably have been excluded from the sample because of the presence of strong emission lines.

iii) The UVK Colors

Figure 4a presents a considerably different picture than Figure 2. First of all only a couple of the Sc nuclei overlap the globular cluster region and less than half overlap the elliptical

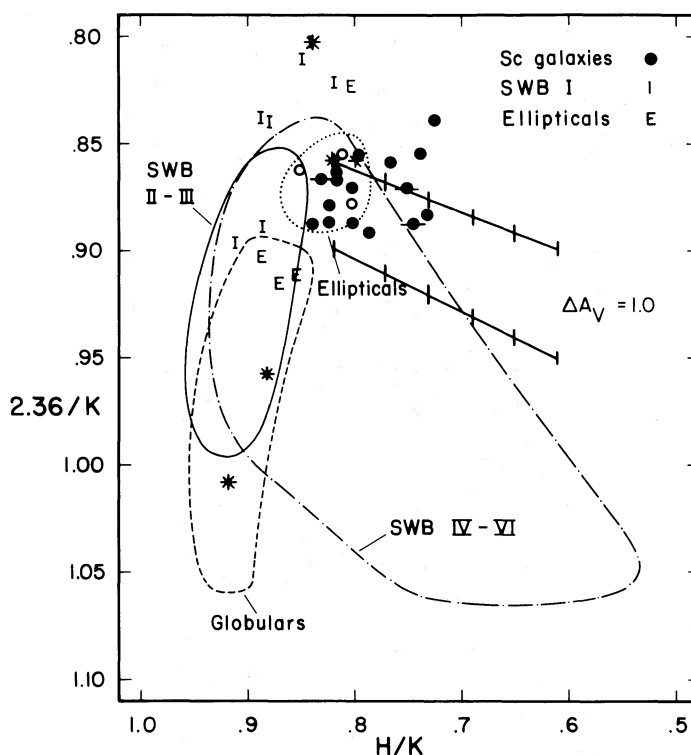


FIG. 6.—Same as for Fig. 5 except that the M15 point is shown explicitly. It is the one with the largest value of $2.36/K$.

galaxy region. Nearly one-third of the galaxies in the Sc sample have K/V values greater than any of the stellar systems shown in Figure 4. Also the bifurcation first noted by Aaronson (1978) is apparent: about five or six galaxies of the present sample have U/V values greater than those of ellipticals or globular clusters with the same K/V .

The V light of the Sc nuclei which lie below the globular-elliptical sequences in Figure 4 could have a substantial contribution from stars of the type found in SWB IV–VI clusters. The fraction of V light from the youngest groups, SWB I–III, is less, in the mean, than the fraction of B light from these same groups.

One obvious explanation for the Sc nuclei with large values

of K/V is internal extinction. If a value for the internal extinction of 1–1.5 mag is allowed for these three nuclei as is suggested by Turnrose's (1976) analysis of similar galaxies, then their intrinsic UVK colors would be consistent with a significant fraction of the light coming from SWB IV–VI type clusters and would require a contribution from the younger groups as well. No contribution from a globular cluster population would be required.

b) Quantitative Examples

Table 8A gives the normalized energy distributions for five different representative objects. Their locations in Figures 2, 4, 5, and 6 are indicated by asterisks. The quantities listed for

TABLE 8A
NORMALIZED ENERGY DISTRIBUTIONS

Object	Type	U	B	V	J	H	K	$2.36 \mu\text{m}$
M15	MPG	0.59	0.58	1.0	3.31	5.11	5.55	5.60
NGC 1805	I	1.75	0.99	1.0	5.81	11.07	13.18	
NGC 1854	II–III	1.24	0.93	1.0	2.27	3.34	3.77	3.63
NGC 2173	IV–VI	0.38	0.49	1.0	6.03	12.59	15.70	13.49
NGC 4472	E	0.24	0.43	1.0	9.29	17.54	21.28	18.20

TABLE 8B
RELATIVE FLUX CONTRIBUTIONS

Objects	B	V	H	K
2173/M15	0.5	0.6	1.46	1.68
4472/M15	0.5	0.68	2.32	2.59
2173/1854	1.06	2.0	7.54	8.32
4472/1854	0.46	1.0	5.25	5.64
2173/1805	1.98	4.0	4.55	4.76
4472/1805	0.86	2.0	3.16	3.22
4472/2173	0.88	1.0	1.39	1.36

each wavelength, X , are just $10^{-0.4(X-V)}$. Data for M15, the metal-poor globular cluster (MPG), are from ACMM. Its location is shown only on Figures 2 and 6. While interpreting these figures it is important to keep in mind that if the relative contribution of a particular representative object to wavelength X is determined from any one of the figures, its relative contribution to the other wavelengths is fixed by the values in Table 8A. Table 8B gives, for various pairs of objects, their relative contributions at the four wavelengths of Figures 2, 4, 5, and 6. These relative contributions are normalized to a particular wavelength for purposes of the examples which now follow.

A simple two component model shows that *the infrared colors effectively rule out any significant contribution from metal-poor globulars to the blue light of Sc nuclei*. Consider the contribution of MPGs to the blue light. Let the Sc nuclei in Figure 2 be dereddened by an amount corresponding to $A_V = 0.5$ –1.0. Then if MPGs contribute significantly to the blue light, the rest of the B light has to come from something much redder, i.e., larger V/B . Let this be a typical old metal-rich population such as that of an E galaxy. Table 8B then shows that if MPGs contribute two-thirds of the B light and Es one-third, then at K the Es can contribute only 2.6 times as much as the MPGs. Figure 6 clearly shows that this cannot be the case—if only Es and MPGs are contributing to K , then Es are giving at least 10 times as much light as are the MPGs. One might be tempted to argue that the colors in Figure 6 (and Fig. 5) are caused by a contribution from SWB I clusters as exemplified by NGC 1805. However, inclusion of this type of cluster results in several inconsistencies for the interpretation of Figure 2.

Table 8B and Figure 6 also show that if E galaxy light is replaced by light from stars of intermediate age, e.g., SWB IV–VI clusters, MPGs are still ruled out.

Next consider a possible stellar component of age 10^7 – 10^8 yr—SWB II–III clusters. Figure 4 shows that if such a population is important at V (after dereddening), a second component at V must be from a population with redder $V-K$ colors—larger K/V . Two possibilities are intermediate age and/or old stars (NGC 2173—like or E galaxy—like). In order to estimate from Figure 4 the relative contributions of these components to the V light, the second group of ratios in Table 8B gives the contributions at the other wavelengths. It is easy to verify that these numbers are reasonably consistent with the relative location of the objects in Figure 2, 5, and 6. The only obvious inconsistency is that NGC 2173 light seems to make a somewhat smaller contribution to H and K (Figs. 5 and 6) than is required by the numbers in Table 8B. There is, however enough flexibility in choosing sets of values for representative objects that one could easily remove the inconsistency. Hence both an intermediate and/or old age population fitted equally well when united with a young population in reproducing Sc nuclei light.

Now consider potential contributions from very young stars with ages of a few Myr such as are found in SWB I clusters. As shown in Paper V, such clusters have distinctive $U-V$, $V-K$ colors because of the combined presence of a bright blue main sequence and of luminous red supergiants. We use Figure 4 to first estimate the relative contribution of such a stellar population to the V light. Again 0.5–1.0 mag of internal extinction is assumed. Note that the direction of the extinction tracks in Figure 4 is nearly parallel to the SWB I sequence as it extends to large K/V values. Given the distribution of the galaxy points in this figure, there is a very limited space where an SWB I type

population could contribute as much as half of the V light. If the presence of a typical E galaxy or an SWB IV–VI cluster population is required, then the values given in the third group of numbers in Table 8B are arrived at. If SWB II–III clusters are included, the values do not change much. The locations of objects in Figure 6 could present problems for the inclusion of an NGC 1805 population according to the values in Table 8B. However, in Figure 6, NGC 1805 lies at one extreme of the distribution of SWB I clusters. Choice of a different representative cluster would remove the discrepancy. In summary, then, *a very young stellar population can be a significant contributor to the content of Sc nuclei*. Its contribution, though, could not be more than half that of a somewhat older population characteristic of SWB II–III clusters. If it were as much as half, then exceptionally high star formation rates would be implied.⁴

Can the new data in this paper distinguish between the contributions of intermediate age and old stars as exemplified by SWB IV–VI clusters and E-type galaxies, respectively? In the Magellanic Clouds, half of the bolometric luminosity, on average, of the SWB IV–VI clusters comes from luminous carbon stars (Paper V). As may be seen from Figures 4 and 8a of Paper V, these clusters are spread pretty evenly through the areas assigned to them in Figures 5 and 6 of this paper. The Sc nuclei, on the other hand, occupy rather restricted areas of these latter figures, particularly of Figure 6. An important implication of the locations of the Sc nuclei with respect to the cluster distributions is that *any significant contributions from stars with the colors and luminosities of the C stars found in the SWB IV–VI clusters is ruled out*. In fact, within the errors of measurement, the observed flux ratios and values in Table 8B are consistent with *no* contribution from C stars. Thus an E galaxy-type population is favored over an intermediate-age population.

The dereddened points (the open circles) for the galaxies in common with Turnrose (1976) are in the central part of the E galaxy areas in Figures 5 and 6. Also, as discussed at the end of § Va, nearly all of the Sc nuclei can be moved into the E galaxy regions of Figures 5 and 6 with A_V values less than 1.7, consistent with values derived by Turnrose for his sample. Thus the intrinsic distribution of infrared colors of Sc nuclei may have quite a small dispersion. Hunter and Gallagher (1985) have shown that the JHK colors of a sample of irregular galaxies also have a small dispersion with mean values similar to, but slightly bluer than, those of spiral and elliptical galaxies.

The SWB IV–VI clusters are rather metal-poor (Cohen 1982). It is difficult to predict what the integrated colors of such a cluster would be if they were of solar metallicity which the Sc nuclei probably are. One probable effect would be to sharply reduce the relative number of C to M giants (Renzini and Voli 1981; Iben and Renzini 1983). The increased metallicity of the M giants would make them redder and increase their CO absorption (i.e., smaller values of $2.36/K$). Hence, they might well occupy a more restricted area in Figures 5 and 6. In any case, *an intermediate to old age, metal-rich population is present in probably all of the Sc nuclei studied*; in at least one-third of

⁴ Kennicutt (1983) has used the integrated $H\alpha$ equivalent widths to predict star formation rates (SFRs) for a large sample of spirals. Since his data are averages for entire galaxies, the relatively small nuclei of Sc's would contribute little if anything to the integrated $H\alpha$ line strengths. In any case, there are seven galaxies in common with my sample. For six of these, NGC 157, 628, 1084, 1232, 1385, and 7590, the SFRs range from 6 to $18 M_\odot \text{ yr}^{-1}$. For the seventh, NGC 1637, he calculates an SFR of $0.9 M_\odot \text{ yr}^{-1}$. There is no apparent correlation between his galaxy-averaged SFRs and any of the nuclear specific parameters in Table 4 of this paper.

the sample this stellar population dominates the light from the blue to the infrared.

Finally, there is the question of the effect of thermal emission from heated dust grains on the infrared colors. In an unpublished survey of about 60 bright southern spirals, Frogel, Elias, and Phillips (1985) find that for galaxies with optical emission lines of similar weakness to those in the present sample there is generally no evidence for excess emission at 3.5 or at 10 μm . Willner *et al.* (1984) also failed to find any excess infrared emission in a sample of five weak emission-line spirals. It is unlikely, therefore, that the infrared colors of the galaxies in the present sample are affected by thermal dust emission.

c) The Problem of Internal Extinction

It is difficult to assess the effects of internal reddening on nuclear colors of the Sc galaxies. There are two rather fundamental problems. Most values of A_V are determined at optical wavelengths. It is possible that the extinction applicable to the flux at infrared wavelengths should be considerably greater. Such a situation would arise if the extinction within the measuring aperture were nonuniform or if the obscuring material were mixed in with the stars, both of which are likely occurrences for Sc galaxies. The net effect is that the infrared flux would have a larger contribution from stars with large amounts of extinction than would the optical flux. A second problem is that a normal reddening law may not be applicable to Sc nuclei. In M31 Searle (1983) has found systematic changes in the reddening law with radius. In the M31 nuclear region the reddening law is "dramatically different" from that found for the solar vicinity. Since little can be done to assess these two effects for the galactic nuclei under discussion, the remainder of this paper will assume a normal reddening law with uniform extinction.

An unfortunate coincidence evident from Figures 2 and 4 is that reddening vectors are parallel to the elongated cluster and elliptical galaxy sequences.

One possible estimate of the internal extinction is given in column (3) of Table 4. It is based on the inclination of the galaxy and may or may not be relevant to the nuclear regions. Reddening corrections based on these values were applied to the data. Other than a shifting of all the points in Figures 2–6 back along the reddening vectors and some degree of shuffling, the numerical results contained in Tables 7A–7E were not qualitatively affected. In particular, the correlations (or lack thereof) found among the various colors remained unchanged as did the overall extent of the distribution of points in Figures 2–6.

Turnrose (1976) derived internal extinction values for seven Sc nuclei by comparing model predictions with observed spectral energy distributions. His values are between 1 and 4 times greater than extinction values based on the effects of inclination alone as given by Sandage and Tammann (1981). For three galaxies in common with the present study, NGC 628, 1084, and 1637, Turnrose calculated A_V 's of 0.3, 1.3, and 1.3, respectively. As may be seen, the latter values are several times greater than the values in column (3) of Table 4. Points representing these three galaxies are marked with short horizontal lines in Figures 2–6. The small open circles show their locations after correction for Turnrose's A_V values. Their optical colors (Figs. 2 and 4) then become comparable with those for the bluest galaxies in the sample. Their infrared colors, on the other hand (Figs. 5 and 6), are shifted into the region occupied by most of the other galactic nuclei. Turnrose predicts a

$(V-K)_0$ of 2.8 for NGC 628 on the basis of his models without any *a priori* knowledge of the infrared colors. If the $(V-K)$ value in Table 4 is corrected for Turnrose's suggested internal $E(B-V)$ of 0.1, a value of 2.7 is arrived at. Such agreement is encouraging.

As an experiment, the dereddened $J-H$ colors of all of the Sc nuclei were assumed to be equal to 0.65 (or $J/H = 0.55$)—a value which seems reasonable on the basis of Figure 5. For each galaxy a value of A_V was calculated and all of the colors corrected. The calculated A_V values ranged between 0.0 and 1.64 mag. Differences that might arise if the dust were mixed in with the stars rather than lying in a uniform absorbing layer were ignored. The right-hand panels of Figures 2 and 4 show the effects of this dereddening on the $UBVK$ colors. Although there has been a general shifting of the points to bluer colors in Figure 2, the dispersion has remained the same in this figure while it has been considerably reduced in K/V (Fig. 4) as expected from the lack of correlation between optical and infrared colors.

It is clear from Figure 2b that SWB II–III type stars are now contributing half of the B light in many of the nuclei. Table 8B and the other flux ratio plots are entirely consistent with this result if the remaining B light comes from some combination of E galaxy and SWB IV–VI cluster light.

VI. SUMMARY AND CONCLUSIONS

Blue stars from young stellar systems such as Magellanic Cloud clusters of SWB type I–III (age $\lesssim 100$ Myr) make a significant contribution to the optical light of many of the Sc nuclei in the present sample. The infrared light, on the other hand, is dominated by an older and probably metal-rich stellar population such as is found in Magellanic Cloud clusters of SWB type IV–VI (age \approx a few Gyr) and/or elliptical galaxies. Neither the optical nor the infrared data permit any significant contribution to the light of Sc nuclei from old, metal-poor stellar systems as claimed by CCM. O'Connell (1982, 1983) and Turnrose (1976) have also concluded that in the optical the nuclear light of Sc's can best be understood as the superposition of metal-rich stellar populations of various ages. O'Connell (1982, 1983) discusses possible reasons why these conclusions are so discrepant from those of CCM.

The infrared colors of the Sc nuclei are not correlated with their optical colors and both are only weakly correlated with the absolute blue magnitudes of the galaxies. Large galaxy-to-galaxy variations in the optical colors of the nuclei reflect significant variations in the present (i.e., averaged over the past 100 Myr) rate of star formation. On the other hand, the close similarity of the infrared colors of the Sc nuclei indicates a degree of uniformity in the older stellar population.

A comparison of the UBV colors of the Sc nuclei with the models of Searle, Sargent, and Bagnuolo (1973) and of Larson and Tinsley (1978) suggests that in some of the nuclei star formation has occurred continuously since birth, while in others it has occurred in bursts which in some cases have been strong enough to permit the young stars to dominate the optical light. This is so even though strong emission-line galaxies were excluded from the sample. As Searie *et al.* and Huchra (1977) have concluded, there are no young galaxies, only ones with varying amounts of current star formation. The change in the location of the Sc nuclei sequence relative to the cluster and early-type galaxy sequences as one goes from blue wavelengths to the red is a reflection of the fact that the pre-

sence of red stars in a composite system will be most obvious in the infrared (Paper I; Aaronson 1978).

The relative contribution of the youngest stars, those from clusters of SWB I type, to the optical light of the Sc nuclei cannot be more than half that from the somewhat older SWB II–III group. However, the relative contribution of the former type of star to the infrared colors can be twice that of the latter. This is because of the presence of many red supergiants in SWB I clusters (Paper V).

Clusters whose bolometric luminosity and infrared colors are dominated by luminous carbon stars, such as many of the ones of SWB types IV–VI in the Magellanic Clouds, do *not* make any significant contribution to the integrated light of the Sc nuclei in the present study. There are, though, a few Cloud clusters of these types which are dominated by luminous M giants rather than C stars. NGC 2162 and 2173 are two examples (Paper V). These clusters, however, are the exception rather than the rule among the SWB IV–VI population. A stellar population of such clusters could dominate the infrared light and be a major contributor to the optical light of the Sc nuclei. Our current understanding of the evolution of cool giants would allow the production of such a C star-poor, M star-rich intermediate-age population in a more metal-rich environment than that which existed in the Magellanic Clouds when clusters of similar age formed. Thus, on the basis of the present data alone a clear distinction cannot be made between the contribution of an elliptical galaxy-type population and that of an M star-dominated cluster of SWB types IV–VI. Nonetheless, it seems somewhat less contrived to conclude that the infrared light of the Sc nuclei is dominated by a stellar population similar to that found in elliptical galaxies.

There is indirect evidence of considerable—up to 1.6 mag—extinction internal to the Sc nuclei. This extinction is, in many cases, greater than and uncorrelated with extinction values derived from galaxy inclination angles. Values for A_V derived from model fitting (Turnrose 1976) are consistent with the data presented in this study.

For elliptical and lenticular galaxies there is a correlation between high luminosity and red colors, both optical and infrared. Such a correlation is usually interpreted as arising from decreasing metallicity in the fainter galaxies (i.e., Faber 1973). Two of the three optically bluest galaxies in Table 4 (NGC 247 and 7793) are also the two faintest. (Note, though, that the

nuclear magnitude of NGC 7793 [Table 1] is not particularly faint.) But their positions in Figures 2, 3, and 4 imply that their blue colors are primarily due to a young population rather than a metal-poor one. Similarly, Hunter and Gallagher (1985) have failed to detect a correlation between luminosity and infrared color in a sample of blue irregular galaxies.

The $U - V$ and $V - K$ colors of Sc galaxies get strongly redder with decreasing central distance. Although these color gradients are much steeper than those found within early-type galaxies, the ratios of the two gradients is the same as the slope of the $U - V$, $V - K$ relation for the integrated colors of E and S0 galaxies. This slope, in turn, differs only slightly from that which obtains for globular clusters. In the case of globular clusters and early-type galaxies, the color-color relation is usually interpreted as arising primarily from metallicity differences; in particular, from a blueward shift of the giant branch in the case of $V - K$ and from a blueward shift of the subgiants and main-sequence stars in the case of $U - V$.

The situation for late-type spirals is considerably more complex. First of all it is clear that within spiral nuclei there are significant numbers of stars with a range in ages probably as great as the age of the galaxy itself. Also there appears to be a considerable amount of reddening material within the nuclear region. The major complexity, though, may be the fact that as the size of the measuring aperture is increased so does the relative contribution to the light from disk stars. Thus, it is surprising that $(U - V)/(V - K)$ ratio within spirals is so close to that between early-type systems. (Although the $U - V$ and $V - K$ colors between spirals is highly correlated [Tables 7B and 7C], it is obvious from Figure 4 that the nature of this correlation is quite different from that which obtains for early-type systems). The agreement may just be fortuitous—there are, after all, only five spirals in Table 5 with established $V - K$ gradients. An investigation of population gradients within spiral nuclei based on both photometric and spectroscopic data in the optical and infrared would be the next logical step.

Critical readings of a draft of this paper by Roger Davies and Jay Gallagher led to significant improvements in the presentation. Pat Osmer and Leonard Searle made a number of useful suggestions. A conversation with Mark Phillips helped to clarify for me the characteristics of different types of emission-line galaxies.

REFERENCES

- Aaronson, M. 1977, Ph.D. thesis, Harvard University.
 ———. 1978, *Ap. J. (Letters)*, **221**, L103.
 Aaronson, M., Cohen, J., Mould, J., and Malkan, M. 1978, *Ap. J.*, **223**, 824 (ACMM).
 Aaronson, M., Frogel, J. A., and Persson, S. E. 1978, *Ap. J.*, **220**, 98 (Paper II).
 Alcaïno, G. 1974, *Astr. Ap. Suppl.*, **13**, 305.
 Alloin, D. 1973, *Astr. Ap.*, **27**, 433.
 Bevington, P. R. 1969, *Data Reduction and Error Analysis for the Physical Sciences* (New York: McGraw-Hill).
 Cohen, J. G. 1982, *Ap. J.*, **258**, 143.
 Cohen, J. G., Frogel, J. A., Persson, S. E., and Elias, J. H. 1981, *Ap. J.*, **249**, 481.
 Cowley, A. P., Crampton, D., and McClure, R. D. 1982, *Ap. J.*, **263**, 1 (CCM).
 Deeming, T. J. 1964, *M.N.R.A.S.*, **127**, 35.
 de Vaucouleurs, G., and de Vaucouleurs, A. 1972, *Mem. R.A.S.*, **77**, 1.
 de Vaucouleurs, G., de Vaucouleurs, A., and Corwin, M. G. 1978, *A.J.*, **83**, 1331.
 Diaz, A. I., Pagel, B. E. J., Edmunds, M. G., and Phillips, M. M. 1982, *M.N.R.A.S.*, **201**, 49P.
 Elias, J. H., Frogel, J. A., Matthews, K., and Neugebauer, G. 1982, *A.J.*, **87**, 1029.
 Faber, S. M. 1973, *Ap. J.*, **179**, 731.
 Frogel, J. A., Elias, J. H., and Phillips, M. M. 1985, unpublished.
 Frogel, J. A., Persson, S. E., Aaronson, M., and Matthews, K. 1978, *Ap. J.*, **220**, 75 (Paper I).
 Frogel, J. A., Persson, S. E., and Cohen, J. G. 1980, *Ap. J.*, **240**, 785 (Paper IV).
 Glass, I. S. 1973, *M.N.R.A.S.*, **163**, 35P.
 Heckman, T. M. 1980, *Astr. Ap.*, **87**, 142.
 Hodge, P. W. 1983, *Publ. A.S.P.*, **95**, 721.
 Huchra, J. P. 1977, *Ap. J.*, **217**, 928.
 Hunter, D. A., and Gallagher, J. S., III. 1985, *A.J.*, in press.
 Iben, I., Jr., and Renzini, A. 1983, *Ann. Rev. Astr. Ap.*, **21**, 271.
 Keel, W. C. 1983, *Ap. J. Suppl.*, **52**, 229.
 Kennicutt, R. C., Jr. 1983, *Ap. J.*, **272**, 54.
 Landolt, A. U. 1973, *A. J.*, **78**, 959.
 Larson, R. B., and Tinsley, B. M. 1978, *Ap. J.*, **219**, 46.
 Morgan, W. W. 1962, *Ap. J.*, **135**, 1.
 O'Connell, R. W. 1982, *Ap. J.*, **257**, 89.
 ———. 1983, *Ap. J.*, **267**, 80.
 Olson, B. I. 1975, *Pub. A.S.P.*, **87**, 349.
 Persson, S. E., Aaronson, M., Cohen, J. G., Frogel, J. A., and Matthews, K. 1983, *Ap. J.*, **266**, 105 (Paper V).
 Persson, S. E., Frogel, J. A., and Aaronson, M. 1979, *Ap. J. Suppl.*, **39**, 61 (Paper III).
 Phillips, M. M. 1984, private communication.

- Rabin, D. M. 1980, Ph.D. thesis, California Institute of Technology.
Renzini, A., and Voli, M. 1981, *Astr. Ap.*, **94**, 175.
Sandage, A. R. 1972, *Ap. J.*, **176**, 21.
Sandage, A., and Tammann, G. A. 1981, *A Revised Shapley-Ames Catalog of Bright Galaxies* (Washington, D.C.: Carnegie Institution of Washington).
Searle, L. 1983, in *Ann. Rept. Carnegie Institution of Washington for 1982-1983*, p. 622.
Searle, L., Sargent, W. L. W., and Bagnuolo, W. G. 1973, *Ap. J.*, **179**, 427.
Searle, L., Wilkinson, A., and Bagnuolo, W. G. 1980, *Ap. J.*, **239**, 803 (SWB).
Shobbrook, R. R. 1966, *M.N.R.A.S.*, **131**, 351.
Turnrose, B. E. 1976, *Ap. J.*, **210**, 33.
van den Bergh, S. 1969, *Ap. J. Suppl.*, **19**, 145.
———. 1981, *Astr. Ap.*, **46**, 79.
Whitford, A. E. 1971, *Ap. J.*, **169**, 215.
———. 1978, *Ap. J.*, **226**, 777.
Willner, S. P., Ward, M., Longmore, A., Lawrence, A., Fabbiano, G., and Elvis, M. 1984, *Pub. A.S.P.*, **96**, 143.

JAY A. FROGEL: NOAO, P.O. Box 26732, Tucson, AZ 85726